Materials Science & Engineering A 612 (2014) 187–191

Contents lists available at ScienceDirect

Materials Science & Engineering A

journal homepage: www.elsevier.com/locate/msea

Rapid communication

Tailoring texture and refining grain of magnesium alloy by differential speed extrusion process

Qingshan Yang [a,b], Bin Jiang [a,b,*], Junjie He [a], Bo Song [c], WenJun Liu [a], Hanwu Dong [a,b], Fusheng Pan [a,b]

[a] College of Materials Science and Engineering, National Engineering Research Center for Magnesium Alloys, Chongqing University, Sha Zheng Jie 174#, Chongqing 400044, China
[b] Chongqing Academy of Science and Technology, Chongqing 401123, China
[c] Faculty of Materials and Energy, Southwest University, Chongqing 400715, China

ARTICLE INFO

Article history:
Received 24 August 2013
Received in revised form
12 June 2014
Accepted 14 June 2014
Available online 20 June 2014

Keywords:
Mg alloy
Microstructure
Mechanical properties
Texture
Extrusion

ABSTRACT

Magnesium alloy sheets were processed by conventional extrusion (CE) and differential speed extrusion (DSE). The velocity evolutions of DSE sheets at near-surface and mid-layer region are different due to the extra asymmetric shear deformation. This simple shear enforces the near-surface microstructure to exhibit more dynamically recrystallized grains having the *c*-axis tilted about $\pm 12^\circ$ toward the extrusion direction. Grain refinement and tilted weak basal texture obtained by DSE process dramatically enhance the room temperature strength and plasticity of the extruded Mg alloy sheets.

1. Introduction

Magnesium alloy is one of the lightest metallic materials in the area of structural applications. Mg alloys have brought significant advances in the automotive industry and electronic products due to their high specific properties [1,2]. Manufactures of Mg alloys mostly focus on strip and sheet productions which can be expanded for the fabrication of structural components [3,4]. The dominant slip system of Mg alloy is slip in the close packed direction $\langle 11\bar{2}0\rangle$ or $\langle a\rangle$ on the (0002) basal plane at room temperature [5,6]. Mg alloy sheet usually yields a strong basal texture during the severe plastic deformation (SPD) processes such as extrusion and rolling, which in turn bring about the limited room temperature formability related to their hexagonal close-packed (hcp) crystal structure [7,8].

Texture control should be considered as an effective way to enhance the formability during the primary processing. It is of significant interest to explore the mechanical response and deformation mechanism guidelines for designing the relevant devices. Extrusion process has been applied as an economical way to produce the sheet fabrication for the structural components [9–11]. However, conventionally extruded Mg alloy sheets possess poor mechanical properties due to the strong basal texture where *c*-axes of the grains are predominantly aligned parallel to the sheet normal direction. This brings about a poor deformation capability of sheet thinning and a stronger anisotropy and consequently results in a limited number of available plastic deformation modes [12]. There were a great many technologies aimed to modify the texture of Mg alloy sheets characterized by the inclination direction, the tilted angles of the basal plane and the texture intensity, e.g. equal-channel angular pressing (ECAP) [13], differential speed rolling (DSR) [14], alloying [15] and heat treatment [16]. Differential speed rolling (DSR) has actively altered the final texture which helps in modifying the mechanical properties of the rolled sheets. The velocity between the top and bottom rolls is different in DSR process. It creates the asymmetric shear deformation in the whole thickness of the sheets [17,18]. This differential speed processing is expected to introduce a single extrusion step of strain paths associated with the novel integrated process in one pass. Inspired by the DSR process, in the present work, a superior process of differential speed extrusion is established to ameliorate the texture-dependent mechanical properties of Mg alloy sheets.

2. Experimental procedure

The starting material was a hot-extruded AZ31 (Mg–3Al–1Zn in wt%) alloy sheet with a thickness of 1 mm. The extrusions were

---

* Corresponding author at: College of Materials Science and Engineering, National Engineering Research Center for Magnesium Alloys, Chongqing University, Sha Zheng Jie 174#, Chongqing 400044, China. Tel./fax: +86 23 65111140.
E-mail address: jiangbinrong@cqu.edu.cn (B. Jiang).

http://dx.doi.org/10.1016/j.msea.2014.06.045
0921-5093/

respectively conducted by the conventional extrusion (CE) and the differential speed extrusion (DSE) dies at 430 °C with an extrusion ratio of 101:1. The extrusion rate was maintained at 20 mm/s. The extruded AZ31 alloy sheets were of 56 mm width (transverse direction, TD) and 1 mm thickness (normal direction, ND).

Dog-bone tensile samples of 12 mm in gage length, 6 mm in width and 1 mm in thickness were machined from the sheets with various directions tilting 0°, 45° and 90° to the extrusion direction (ED), respectively. Tensile tests were performed on a CMT6305-300KN universal testing machine at the initial strain rate of $10^{-3}\,s^{-1}$ at room temperature. The electron backscatter diffraction (EBSD) data was collected using an HKL Chanel 5 System equipped FEI Nova 400 FEG-SEM. The analysis of (0002) pole figures was determined using X-ray diffraction (Rigaku D/Max 2500). For the DSE sheets, the pole figures and EBSD orientation maps were measured at top surface, mid-layer (ND, 0.5 mm in thickness was removed from the surface) and bottom surface, respectively.

3. Results and discussion

Fig. 1 shows the schematic section of flow passage in CE and DSE dies. The velocity of the top and bottom surfaces is the same because of a symmetric plane during CE process. DSE die is equipped with a different parallel flow passage length ($L=4$ mm). The shear strain deformation results from a difference in velocity between the top and bottom surfaces of the extruded sheets. This leads to the asymmetric shear strain deformation in the sheet thickness direction in one pass during the extrusion processing. The finite element model (FEM) was employed to examine the effective strain and velocity distribution of the Mg alloy sheets during these processes. The flow stress data of AZ31 Mg alloys were imported into the commercial finite element software. For an easier comprehension of the extrusion process, CE process was also analyzed to compare the results with those of DSE process. The FEM simulations in terms of the effective strain and the velocity distribution of Mg alloy at top and bottom layers as a function of distance from the entrance are presented in Fig. 2. The curve represents the change of the effective strain and velocity in the whole extrusion for the AZ31 workpiece. It can be seen that the effective strain and the velocity distribution in both layers are nearly the same in CE process (Fig. 2a, b, e and f), while there exists a strain and velocity gradient in the DSE process (Fig. 2c, d, g and h). The effective strain and velocity gradually increased from the entrance toward the exit of the deformation zone. Meanwhile, the value of strain and velocity at top surface is higher in DSE. The velocity ratio between the top and bottom surfaces is about 2:1. DSE process is efficient in producing plastic deformation since it develops additional shear strain for a given reduction in the thickness direction (ND). It presents the total effective strain accumulated in the layers, as well as the average and maximum deviation. Thus, the peaks would appear. It shows the maximum value at this time. It can be indicated that the top surface would produce the greatest maximum deviation and the bottom surface would produce the least average.

Fig. 3 shows the (0002) pole figures and EBSD orientation maps of the CE and DSE samples (at top surface, mid-layer and bottom surface) in detail. CE sheets are characterized by homogeneous microstructure with equiaxed dynamically recrystallized (DRX) grains of approximately 12 μm. It is found that a considerable grain refinement is accomplished by DSE process. The grain refinement mechanism was mainly due to the grain subdivision in order to accommodate the intense plastic strain by DSE deformation [18]. Top surface (DSE_t) microstructure of the DSE sheet is depicted in Fig. 3(b). Here, the DRX grains seem to be little finer (~7 μm) than those of CE sheets. Elongated deformed grains of 15–33 μm are embedded in a matrix of fine grains (~10 μm) in the mid-layer (DSE_m) microstructure. The large elongated grains of DSE_m were thought to have survived from the recrystallization during the DSE process due to the difference of strain deformation in ND. As shown in Fig. 3c, the grains of DSE_m are elongated along the imposed shear deformation direction. The bottom surface (DSE_b) microstructure reveals the DRX grains of ~8 μm in Fig. 3d. As mentioned earlier, simulation results indicate that the velocity and effective strain of DSE_t are higher. The finer DRX grains of DSE_t were suggested to form under the present shear strain path. It transforms subgrain boundaries in the mantle regions of elongated grains (high stress concentrations) into high angle boundaries [19]. The DSE sheet also possesses different textural features which include the inclination direction, the rotated angle of the basal plane and the texture intensity in the through-thickness direction (ND). The texture of CE sheets was characterized as a strong splitting of pronounced basal texture after the hot-extrusion process, and there was no obvious difference from the texture of generally rolled AZ31 alloy sheets [20,21]. In contrast, the (0002) basal texture of the DSE sheet has been weakened and tilted towards ED compared with the one in CE sheet. The grains of the DSE sheets are elongated and rotated away from the basal plane because of the imposed shear deformation [22,23]. This makes the basal plane rotated towards the imposed

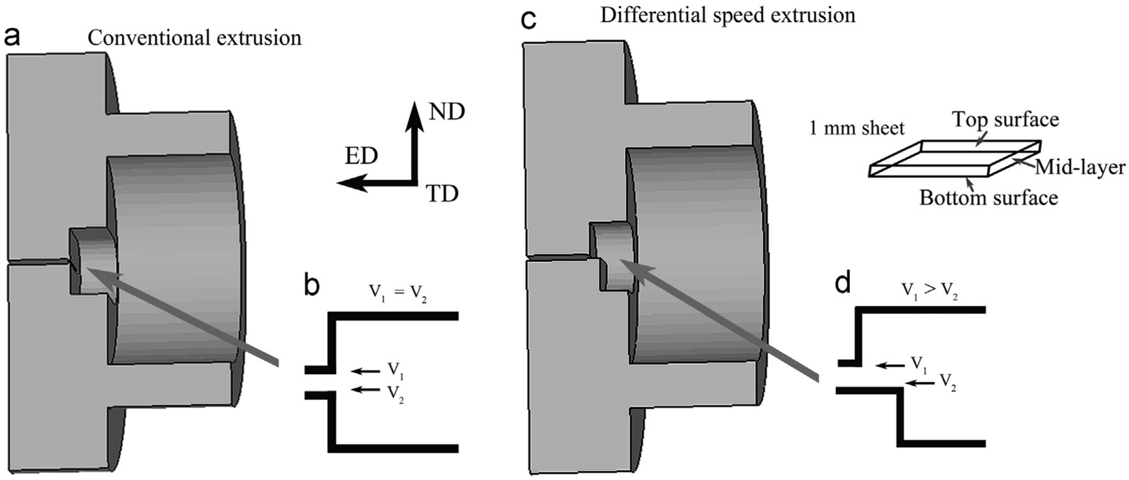

Fig. 1. Schematic sectional view of the conventional extrusion die (a) and the differential speed extrusion die (c). Illustration of the flow passage in the conventional extrusion die (b) and the differential speed extrusion die (d) in details.